Food Hydrocolloids 147 (2024) 109310

Contents lists available at ScienceDirect

Food Hydrocolloids

journal homepage: www.elsevier.com/locate/foodhyd

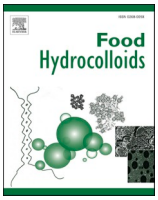

Bacterial nanocellulose spheres coated with meta acrylic copolymer: *Vaccinium meridionale swartz* extract delivery for colorectal cancer chemoprevention

M. Osorio [a,b], L. Posada [a], E. Martínez [a], V. Estrada [b], G. Quintana [a], Maria E. Maldonado [c], S. Peresin [d], J. Orozco [e], C. Castro [a,*]

[a] School of Engineering, Universidad Pontificia Bolivariana, Circular 1 No. 70-01, Medellín, Colombia
[b] School of Health Science, Universidad Pontificia Bolivariana, Calle 78b No. 72 A-109, Medellín, Colombia
[c] Nutrition and Dietetic School, University of Antioquia, Carrera. 75 No. 65-87, Medellín, Colombia
[d] Biomaterials Chemistry and Nanotechnology, Auburn University, 23 Samford Hall, Auburn, AL, 36849, USA
[e] Max Plack Tadem Group in Nanobioengineering, Universidad de Antioquia, Complejo Ruta N, Torre A, Laboratorio 4-166, Calle 67 No. 52-20, Medellín, 050010, Colombia

ARTICLE INFO

Keywords:
Bacterial nanocellulose
Vaccinium meridionale swartz extract
Meta-acrylic copolymer
Drug delivery systems
Colorectal cancer
Functional food ingredients
Phytochemicals

ABSTRACT

Bacterial nanocellulose, a natural hydrocolloid traditionally used as food ingredient, has demonstrated potential as a non-soluble dietary fiber and functional material. Moreover, its properties can further be potentialized whether coupled with natural anthocyanins to endow antioxidant activity. *Vaccinium meridionale swartz* extract (VE), rich in anthocyanins, has recently demonstrated effects against colorectal cancer; therefore, encapsulating it into bacterial nanocellulose (BNC) may offer an enhanced VE delivery alternative. However, BNC has an open interconnected porosity that may generate a quick delivery of VE in gastric fluids impacting its stability. Accordingly, this paper explores meta-acrylic copolymer coatings of BNC spheres for VE delivery in a colorectal environment while potentially reducing its delivery in stomach conditions. The VE was characterized in terms of antioxidant capacity, colorectal cancer cell inhibition, and selectivity and then, it was incorporated into BNC spheres and coated with a meta-acrylic copolymer. The system's physicochemical, morphological, and delivery performance was studied under colonic and gastric conditions. Results show the coating's effectiveness in changing the VE delivery profile under colonic conditions and the potential of natural extracts for the selective inhibition of colorectal cancer cells (SW480 and SW620). The above results demonstrated that meta-acrylic copolymer-coated BNC spheres is a potential system for encapsulating natural extracts for colorectal cancer chemoprevention.

1. Introduction

Bacterial nanocellulose (BNC) is a natural hydrocolloid produced by bacteria from the genus *Komagataeibacter*, *Gluconacetobacter*, among others, as a thick mat or membrane in the air-liquid interface under static fermentation with carbon and nitrogen sources (Martínez Ávila et al., 2014). These bacteria may form entangled nanoribbons networks of 50–70 nm in width and several microns in length (Kumagai et al., 2011) during BNC biosynthesis (Martínez Ávila et al., 2014), (Kumagai et al., 2011) BNC shares the chemical structure of other vegetable and animal cellulose sources, i.e., chains of D (+) glucose $(C_6H_{10}O_5)_n$ linked by β 1–4 bounds (Azeredo et al., 2019a), Azeredo et al., 2019a,b but it is highly pure (Kim et al., 2011a; Trovatti et al., 2011; Yudianti & Karina, 2012), and has historically used as food and food ingredient (Azeredo et al., 2019a), (Osorio et al., 2017). BNC was first observed by ancient Asians producing kombucha tea (Jarrell et al., 2000), a beverage fermented from a symbiotic colony of acetic acid bacteria and yeast embedded within a nanocellulose membrane formed at the beverage surface (Azeredo et al., 2019a), (Jarrell et al., 2000). Likewise, BNC is produced in coconut water in the Philippines to harvest "*nata de coco*" (Martínez Ávila et al., 2014), (Recouvreux et al., 2011), (Zhu, Jia, et al., 2011) as a dessert and food ingredient of beverages (Okiyama et al., 1993). Moreover, BNC is generally recognized as safe (GRASS) by the Food and Drug Administration (FDA), and it has been exploited as a raw

* Corresponding author.
E-mail address: cristina.castro@upb.edu.co (C. Castro).

https://doi.org/10.1016/j.foodhyd.2023.109310
Received 21 February 2023; Received in revised form 28 August 2023; Accepted 18 September 2023
Available online 25 September 2023

material for dessert, artificial meat, thickening, gelling, and water-binding agent, and food packaging material, among others (Shi et al., 2014).

BNC can be shaped during biosynthesis to generate fibrous suspension, spheres, or pellets (Azeredo et al., 2019a). Using agitated culture BNC can be shaped into spheres (also reported as pellets, beads, or cocoon-like spheroids) in sizes varying from microns to centimeters in diameter (Recouvreux et al., 2011)– (Czaja et al., 2004). The production mechanism of these shapes is still unknown; however, it is influenced by the cultivation time and agitation speed (Czaja et al., 2004). In this context, BNC spheres have been produced for soft tissue regeneration (Czaja et al., 2004) and the adsorption of proteins and heavy metals (Zhu et al., 2011b), For instance Pb^{2+}, Mn^{2+}, and Cr^{3+} have been removed from effluents demonstrating high adsorption and recyclable capacities (Recouvreux et al., 2011), (Zhu, Jia, et al., 2011), (Zhu et al., 2011b), (Brandes et al., 2018). Moreover, BNC has been used as encapsulation material for colorectal cancer, rencently estudies of Martinez et al. (2022), Castaño et al. (2022) and Rendon et al. (2022) have used BNC as a drug delivery system for 5-Flourouracil and genistein demonstrating its potential for promoting *in vitro* biobility and enhancing inhibition concentration of the encapsulated compounds because of the controlled delivery profile that the compounds presented once were encapsulated on BNC (Castaño et al., 2022; Martínez et al., 2022; Rendón et al., 2022). Likewise, natural extracts from *Vaccinium meridionale swartz* (VE) are a source of polyphenols (antioxidants phytochemicals), especially anthocyanins (delphinidin-3-hexoside, cyanidin-3-galactoside, cyanidin-3-arabinoside, among others), and flavonols (quercetin hexoside, quercetin pentoside, quercetin hydroxymethylglutaryl-α-rhamnoside, among others), the whole composition was described by Garzon et al. (2020) (Garzón et al., 2020). VE phytochemicals inhibited the growth of HT-29, HCT-116, SW480, and SW620 colon cancer cell lines (Maldonado-Celis et al., 2014a). Likewise, recent studies of Arango-Valera et al. (2022a,b) suggested that VE juices exhibited cell cycle arrest and modulated pro-apoptotic proteins, via an alternative programmed cell death. Furthermore, *in vivo* experiments VE juices decreased aberrant crypt foci, and displayed defensive effects against the azoxymethane-induced damage (model that simulates the first steps of colorectal cancer) (Arango-Varela et al., 2022a), the above demonstrates the potential for marketing VE products as nutraceutical food for developing beverages, yogurts, ice creams, among others, with potential colorectal cancer chemopreventive action. VE can be potentiated using BNC, where BNC acts as a delivery system of it. Nevertheless, BNC is an open network (Pircher et al., 2014) that may precociously release VE in the stomach or early intestinal tract impacting its stability and hindering its colorectal cancer effect. To reduce this problem, BNC spheres can be coated with a pH-responsive materials (Shi et al., 2018).

pH-responsive materials get protonated or deprotonated depending on pH (altering the attractive forces between each polymeric chain), showing changes in its swelling behavior. Polimers such as, poly (acrylic acid), poly (methacrylic acid), mehacrylic copolymers, and alginate are materials that are deprotonated at netral to alkaline pH (colon eviroment) (Joseph et al., 2020), allowing the phytochemicals target CRC. Methyl methacrylate copolymers, such as Eudragit S100 (EUDA), is a material that allows colon targeted drug delivery systems (Ratner et al., 2013). For example, EUDA has been investigated as coating agent for tablet formulations of Naproxen (Mehta et al., 2013) and pectin nanoparticles with 5-Flourouracil (Mehta et al., 2013), (Subudhi et al., 2015).

The novelty of this paper lays on the conjuction of the 3 three technologies expressed above, VE chemopreventive properties, BNC as encapsulating agent (responsible for the delivery profile), and EUDA as a pH-responsive coating in order to develop a targeted delivery system for potential CRC chemoprevention, technology that has not been reported in the literature. VE was characterized in its inhibition cancer cells potential, and the whole system (VE encapsulated in BNC coated with EUDA) was physicochemically characterized for potential functional food ingredient to be applyed for colorectal cancer chemoprevention.

2. Materials and methods

2.1. Materials

For *in vitro* studies, high glucose Dulbecco's modified Eagle's medium (DEMEM) (Gibco, 11995065 fetal horse serum (Gibco, 26050070), insulin transferrin selenium 100X (Merck, I3146), non-essential amino acids 100X (Gibco, 11140050), penicillin/streptomycin (Gibco, 15140122), sulforhodamine B (Merck, 230162), and acetic acid (Merck, A6283) were used. For VE characterization potassium chloride (Merck, P3911), sodium acetate (Merck, S2889), 2,4,6-Tri (2-pyridyl)-*s*-triazine (TPTZ) (Merck, T1253), HCl (Merck, 258148), $FeCl_3{\cdot}6H_2O$ (Merck, 236489), and 6-hydroxy-2,5,7,8-tetramethylchromane-2-carboxylic acid (Trolox reagent) (Merck, 238813) were used. For BNC production, D-(+)-glucose (Merck, G5767), potassium dihydrogen phosphate (Merck, P5655), $MgSO_4{\cdot}7H_2O$ (Merck, M5921), disodium hydrogen phosphate (Merck, S9763), and citric acid monohydrate (Merck, C1909), bacteriological peptone (Oxoid, LP0037B), and yeast extract (Oxoid, LP0021B) were used. In addition, the EUDA coating was developed using Eduagrit (Evonik, S100) and ethanol (Merck, 1117272500).

2.2. Vaccinium meridionale Swartz extraction

An adapted protocol from Agudelo-Quintero et al. (2022) was used to produce VE. Briefly, 30 g of ripe lyophilized *Vaccinium meridionale* was reconstituted in 500 ml water. Then it was blended for 5 min, then the mixture was sonicated for 1 h at 25 °C and passed through 0.22 μm Teflon filters (Agudelo-Quintero et al., 2022), after the process the final pH was 3.0. For *in vitro* experiments, the extraction was performed directly, replacing the water for Dulbecco's modified Eagle's medium (DEMEM) at 10 vol % fetal equine serum and 1 vol% insulin transferrin selenium, 1 vol% non-essential amino acids, and 1 vol% of penicillin/streptomycin.

- VE characterization

The VE concentration was calibrated spectrophotometrically, finding a value of 5.63 ± 0.30 mg/ml (gravimetric dry basis). The extraction was characterized in terms of anthocyanin content (main composition and antioxidant activity (Arango-Varela et al., 2022a), (Agudelo--Quintero et al., 2022; Maldonado-Celis et al., 2014b).

Anthocyanins were calculated according to Giusti & Wrolstad, 2001, in which anthocyanin pigments undergo reversible structural transformations with a change in pH manifested by strikingly different absorbance spectra. The colored oxonium form predominates at pH 1.0, and the colorless hemiketal form at pH 4.5. The pH-differential method is based on this reaction and permits accurate and rapid measurement of the total anthocyanins. First, a 0.025 M potassium chloride buffer with pH 1.0 and a 0.4 M sodium acetate buffer with pH 4.5 was used to guarantee the pH. After this, monomeric anthocyanins were measured using UV–visible at 512 nm (Giusti & Wrolstad, 2001). Then, antioxidant activity was measured using the ferric antioxidant/reducing power test (FRAP). This method quantifies the reduction of a ferric tripyridyl triazine (TPTZ) complex to the ferrous form, which has an intense blue color and can be monitored by measuring the change in absorbance at 593 nm. For the method, 300 mM acetate buffer, pH 3.6, was mixed with 10 mM TPTZ (2,4,6-tripyridyl-*s*-triazine) solubilized in 40 mM HCl and 20 mM $FeCl_3{\cdot}6H_2O$ in the ratio of 10:1:1 to give the working FRAP reagent. 900 μl of FRAP reagent, 30 μl of the sample, and 90 μl of distilled water were added to a tube, and the absorbance was read at 593 nm. 6-hydroxy-2,5,7,8-tetramethylchroman-2-carboxylic acid (Trolox reagent) solutions between 20 and 500 μM were used for the calibration curve (Benzie & Strain, 1999). The results are the average of three experiments with its standard deviation.

2.3. Cytotoxic effect of VE on cancer cells

Cell studies were used to prove the inhibition effect of VE over colorectal cancer. The cells tested in the experiment were adenocarcinoma colorectal cancer cells (SW480) and metastatic colorectal cancer cells (SW620), and normal human keratinocytes (HaCaT) as control, using the protocols of Agudelo et al. (2017). Briefly, cells were seeded in 96-well culture plates (Corning, 3598) at 15000 cells per well and cultured using Dulbecco's modified Eagle's medium (DEMEM) at 10 vol % fetal equine serum and 1 vol% insulin transferrin selenium, 1 vol% non-essential amino acids, and 1 vol% of penicillin/streptomycin at 37 °C in 5% CO_2. After 24 h culture, the cells were exposed to 10 concentrations of the VE and incubated for 24 and 48 h. Cell layers were fixed by adding 50 μl of 50 % wt—trichloroacetic acid (TCA) at 4 °C for 1 h. The wells were drained, rinsed with distilled water, and air-dried. Then, the cells were stained using sulforhodamine B (SRB) (0.4% w/v in 1 vol % glacial acetic acid) for 30 min. Unbound dye was drained and removed by washing five times with 1 vol % glacial acetic acid. After air-drying the plate overnight, the dye was solubilized by adding 200 μl/well of 10 mM Tris base and stirring for 10 min, measuring the absorbance at 490 nm. The absorbance of the control group (cells treated with extract solvent) was considered with 100% viability (Carlos et al., 2017). The extent of inhibition was calculated using equation (1).

$$Inhibition = \left[1 - \frac{OD_T}{OD_C}\right] * 100 \quad (1)$$

Where OD_T is the optical density (OD) of treated cells and OD_C is the optical density of control. Furthermore, the selectivity (S) of the compounds was calculated at IC_{50} according to equation (2).

$$S = \frac{IC_{50\,HaCaT}}{IC_{50\,Cancer\ cells}} \quad (2)$$

The IC_{50} parameters were found using 3 replicates in three independent moments, then the outlier point was removed and the data was fitted to a four-parameter Hill equation regression model, according to the procedure followed by Sebaugh, 2010 (Sebaugh, 2011), see equation (3). For the fitting process a non-linear regression (Marquardt) was used. The software for analysis was Statgraphics 19® Centurion.

$$Y = Min + \frac{Max - Min}{1 + \left(\frac{X}{W}\right)^z} \quad (3)$$

Where:

Y is the unitary inhibition.
Min is the minimal asymptote.
Max is the maximal asymptote.
X is the $Log_{10}\ C$ (C is concentration in μg/ml).
W is $Log_{10}IC_{50}$ (IC50 in μg/ml).
Z is the adimentional hill coefficient.

2.4. BNC spheres (BNCS) production

BNCS was produced using a modified Hestrin–Schramm culture media described elsewhere (Molina-Ramírez et al., 2018). First, the pH was adjusted to pH 3.6 with citric acid, and then the medium was sterilized in an autoclave at 15 psi (121 °C) for 15 min. Next, the culture medium was inoculated with *Komagataeibacter medellinensis* at 0.5 Macfarland (1.5×10^8 UFC/ml). Finally, the fermentation was carried out under agitated conditions for 3 days at 30 °C and 150 rpm to generate the BNC spheres using an incubator with agitation (Tecnal, TE-4200). Then, BNC spheres were purified with 5 wt % of KOH solution at room temperature for 14 h, followed by continuous rinsing with ultrapure water to reach a pH of 7.0 (yield of 45 g of BNCS/l).

2.5. VE incorporation

The filtrated was added to 1 g BNCS (wet material) and stirred overnight at 100 rpm in an orbital shaker, according to Table 1.

To form the EUDA coating, the beads with VE (BNC-VE) were immersed in a 2 wt% ethanol solution of EUDA and rinsed in a pH 2 citric acid solution, these compounds were used according to EUDA datasheet and having in mind future application of the thecnology as food aditive. After coating, the spheres were rinsed with ultrapure water (to remove remaning ethanol) and stored for later use. A non-coated experimental group was used to observe the effect of the coating for comparison.

2.6. Material characterization

2.6.1. Macro and microstructurre

The macroscopic appereance of the empty and VE loaded capsules were characterized using a stereomicroscope Nikon at 5X and camera DS-Fi3. For this experemiment, the samples were in its natural state (wet materials). For the characterization of the microstructure a scanning electron microscope (SEM) was used. Futhermore, SEM was used to analyze the morphology of biomaterials before and after coating and VE extract adsorption. First, the samples were frozen at −196 °C using liquid nitrogen. Next, the biomaterials were freeze-dried for 24 h under 0.020 mBar (to preserve the material microstructure and avoiding VE decomposition by temperature); then, the samples were coated with gold using an ion sputter. Finally, samples were observed with a Jeol JSM 5910 LV scanning electron microscope operating at 20 kV.

2.6.2. Attenuated total reflection fourier transform infrared spectroscopy (ATR-FTIR)

ATR-FTIR experiments were carried out to verify the presence of EUDA and extract in the bead. Three samples were freeze-dried before the analysis. Infrared spectroscopy experiments were performed using an FTIR spectrometer (Nicolet 6700 Series) equipped with a single-reflection ATR and a type IIA diamond crystal mounted in tungsten carbide. The diamond ATR had a sampling area of approximately 0.5 mm^2, applying consistent reproducible pressure to every sample. The infrared spectra were collected at 4 cm^{-1} resolutions over 64 scans.

2.6.3. Adsorption profiles

Adsorption isotherms and kinetics were performed to understand the interactions between VE and BNC. All the experiments were performed before the coating of the spheres. The detailed used protocols are described in supplementary information 1 (S.1.)

2.7. Desorption profiles

The coated and uncoated spheres (1 g) with adsorbed VE, BNCS-EUDA-VE, and BNCS-VE, respectively, were immersed in 20 ml of simulated gastric (pH = 1.6) and colonic (pH = 7.0) fluids, according to

Table 1
Experiment set up for adsorption of VE in 1.0 g of BNCS.

Sample No.	W_{VE} (g)	W_{water} (g)	$C_{i,VE}$ (mg/ml)
1	5.0	0.0	4.7
2	4.5	0.5	4.2
3	4.0	1.0	3.8
4	3.5	1.5	3.3
5	3.0	2.0	2.8
6	2.5	2.5	2.3
7	2.0	3.0	1.9
8	1.5	3.5	1.4
9	1.0	4.0	0.9
10	0.5	4.5	0.5

*W: weight (g); C_i: initial concentration (mg/ml); VE: *Vaccinium* Extract.

Marquez et al. 2011 (Marques et al., 2011). Aliquots of 500 μL were taken at 5, 10, 15, 20, 30, 60, 120, and 240 min. The VE concentration was spectrophotometrically analyzed every time, as explained in S.1. for adsorption kinetic. Furthermore, the desorption kinetics were evaluated according to equations in S.1. The fitting of the experimental data was done using the average of the data set in Microsoft Excel® using a non-linear regression (Least Squares) and Solver Complement (Frontline Systems, Inc.).

3. Results and discussion

3.1. VE characterization

Phytochemicals are bioactive nutrient plant chemicals in fruits, vegetables, grains, and other plant foods that may provide desirable health benefits beyond essential nutrition (nutraceutical) to reduce the risk of chronic diseases (Jimenez-Garcia et al., 2018), as cancer. Among the phytochemical family, antocyanins present antioxidant, anti-cancerous, anti-inflammatory, antimicrobial, and vasodilating, among other activities (Yahfoufi et al., 2018). *Vaccinium meridionale Swartz* is a native Colombian plant that produces a dark purple globe berry when it is ripe, rich in anthocyanins with antioxidant properties (Maldonado--Celis et al., 2014a). VE studied here, present an anthocyanins concentration of 57.37 ± 1.51 mg/L cyanidin-3-glucoside and a FRAP antioxidant of 114.94 ± 6.93 of μM Trolox (average and standar deviation). Accordingly, VE presents anthocyanins with antioxidant activity with potential use as a chemopreventive, especially for colorectal cancer. For instance, Baby et al. 2017 reviewed the anti-cancer properties of berries and stated that anthocyanins are quantitatively the most important polyphenolic compound in berries. The quantitative determination of anthocyanin content in strawberries and raspberries ranges from 150 to 600 mg/kg and 921 mg/kg of fresh fruit weight, respectively, showing antiproliferative effects against several cancer cell lines, including breast, colon, and lung, among others (Baby et al., 2017). Conversely, the Andean berries are c. a. of 956 mg/kg of lyophilized fruit, which is relatively high compared to strawberries and in the same range of raspberries, accordingly the anthocyanins concentration and the antiproliferative effect range in similar berries. Likewise, anthocyanin content plays an important role in the antioxidant effect of VE to prevent the free radical damage associated with cancer development (Maldonado, Agudelo, et al., 2017).

3.2. Cell studies of VE over cancer cells

Fig. 1 shows the cell studies over cancer cells (SW480 and SW620) and normal cells (HaCaT).

The inhibitory concentration 50 (IC_{50}) measures the potency or drug efficacy. The results show that cell inhibition exposed to VE is time-, cell-, and dose-dependent. Regarding to time, all cell lines presented better performance of IC50 at 24 h. Regarding the cell type, VE has a lower IC_{50} (most efficacy) for SW480 than for SW620, emphasizing the importance of VE in colon chemoprevention, as this cell line modelled the first colorectal cancer stage (Agudelo-Quintero et al., 2022). Regarding to dose, it was found to have a selective index (SI) above 2.5, meaning that VE is safe for non-cancer cells. For instance, HaCaT IC_{50} is 2-3-fold higher (1000–1500 μg/ml) than for cancer cells (300–500 μg/ml), so that in the inhibitory range of cancer cells, normal cells will not present any cytotoxic effect. There is a wide debate regarding how large the selectivity index should be. Some researchers agree that SI ≥ 10, others >1, or ≥2 or ≥3 (Indrayanto et al., 2021). From the four criteria, the calculated SI agree with three remarking on the safety of VE for inhibiting cancer cells.

In the literature, VE cell inhibition mechanisms have been linked to the antioxidant properties of anthocyanins (114.942 ± 6.928 μM Trolox, found here). Anthocyanins can induce pro-apoptotic events such as activating proteins like caspase-3 and caspase-9 and participating in cytochrome *c* release as Bax and Bak activation and the modulation of nuclear factor kappa B (NF-κB) (Arango-Varela et al., 2022b). Furthermore, NF-κB is mutated in cancer cells (Zhang et al., 2021), which can explain the selectivity of VE, SI > 2.5, compared to non-cancer keratinocytes HaCaT.

Empty capsules of BNCS and BNCS-EUDA were also evaluated *in vitro* showing no effect over cancer and non-cancer cell cells as they no reduced the cell viability, for all cases the viavility was over 90%, please see supplementary information S.2.

3.3. Encapsulation of VE in BNCS and BNCS-EUDA

3.3.1. Material characterization

- Macro and microstructure

Fig. 2 shows the macroscopic appearance of empty capsules BNCS and BNCS-EUDA (Fig. 2 a and b. respectevely) and VE encapsulated, BNCS-VE and BNCS-EUDA-VE (Fig. 2 c and d. respectevely). The developed capsules are characterized by an individualized, dispersed spherical-shaped BNC ranging from 1 to 3 mm in diameter. Once the spheres were coated with EUDA, the spheres keep the macroscopic appereance. When VE is incorporated in the capsules, in both cases the spheres present a vivid and bright color related to VE and the presence of polyphenols in the extract (Carlos et al., 2017), (Celis et al., 2017), that is desired for food or food ingredients (Spence, 2015).

According to Fig. 2, the capsules present the color of anthocyanins (visually attractive), even when it is coated with EUDA (Fig. 2 c. and d.), which is important if VE is intended for functional foods. For instance, bacterial nanocellulose has been used for desserts after being cut into

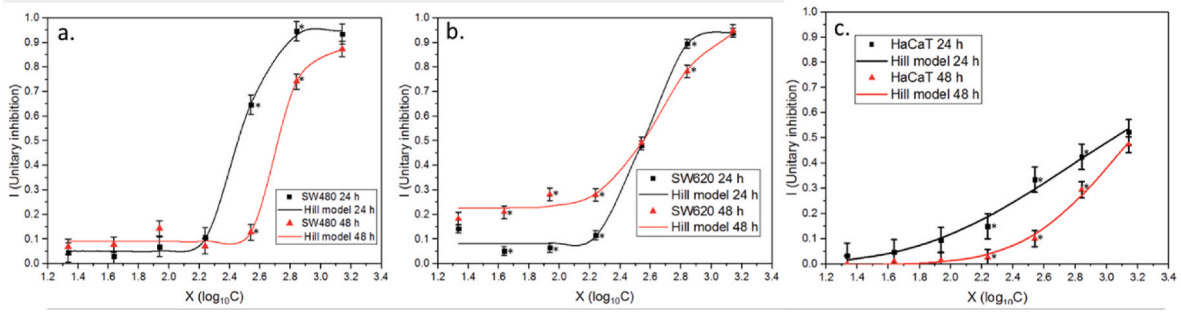

Fig. 1. Inhibitory effect of VE over cancer cells; unitary inhibition vs. X (log_{10} C, C is concentration in μg/mL), along with the Hill model for a. SW480 (primary colorectal adenocarcinoma); b. SW620 (metastatic colorectal adenocarcinoma); c. HaCaT (normal human keratinocytes),*Data points stastiscally different (p-value<0.05). Indented table with: inhibitory concentration 50 (IC_{50}), inferior and superior confidence limit, coefficient of determination (R^2) selectivity index (SI). The adjustment function was symmetric Hill equation using Marquardt regression in Statgraphics, asymptotic intervals with 95% of confidence. N/A means not applicable.

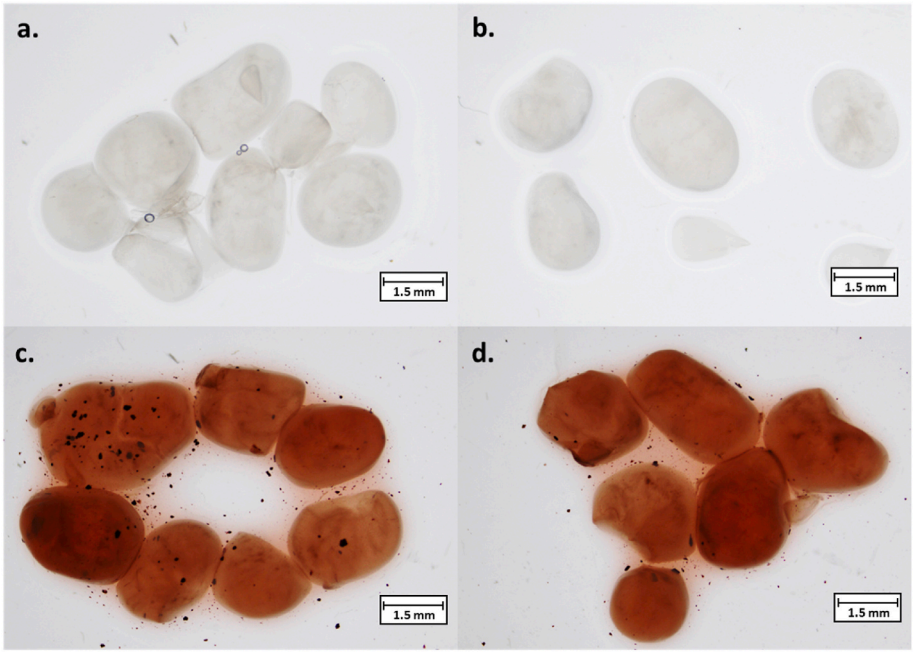

Fig. 2. Macroscopic appearance of the empty capsules and VE encapsulated a. BNCS; b. BNCS-EUDA; c. BNCS-VE; d. BNCS-EUDA-VE. The scale bar represent 1.5 mm.

cubes and immersed in sugar syrup (Azeredo et al., 2019b). Here it is proposed to replace this syrup with VE, which is rich in phytochemicals and has activity against colorectal cancer.

According to the SEM micrograph (see Fig. 3.), the developed spheres with a diameter of c. a. 1.5 mm can be spotted at low magnifications. On the other hand, the BNCS shows the rough structure typical of the material at 500X, given by the interconnected network of nanoribbons (Jarrell et al., 2000). In the case of the BNCS-VE, the nanoribbons are covered by the VE components. Nevertheless, at 10000X, they still present an open porosity (please see arrows), which can quickly release the VE as soon as in contact with simulated fluids, as shown in the desorption analysis. On the contrary, the spheres coated with EUDA present a smooth and wholly closed surface, even at high magnifications, which allows the polymer to act like a drug delivery system, as presented in the following sections.

- FTIR

  Fig. 4 shows the FTIR-ATR spectra of the bacterial nanocellulose spheres. Including its single components, empty capsules and full system. Regarding to VE (see Fig. 4 a.) bands related to anthocynis

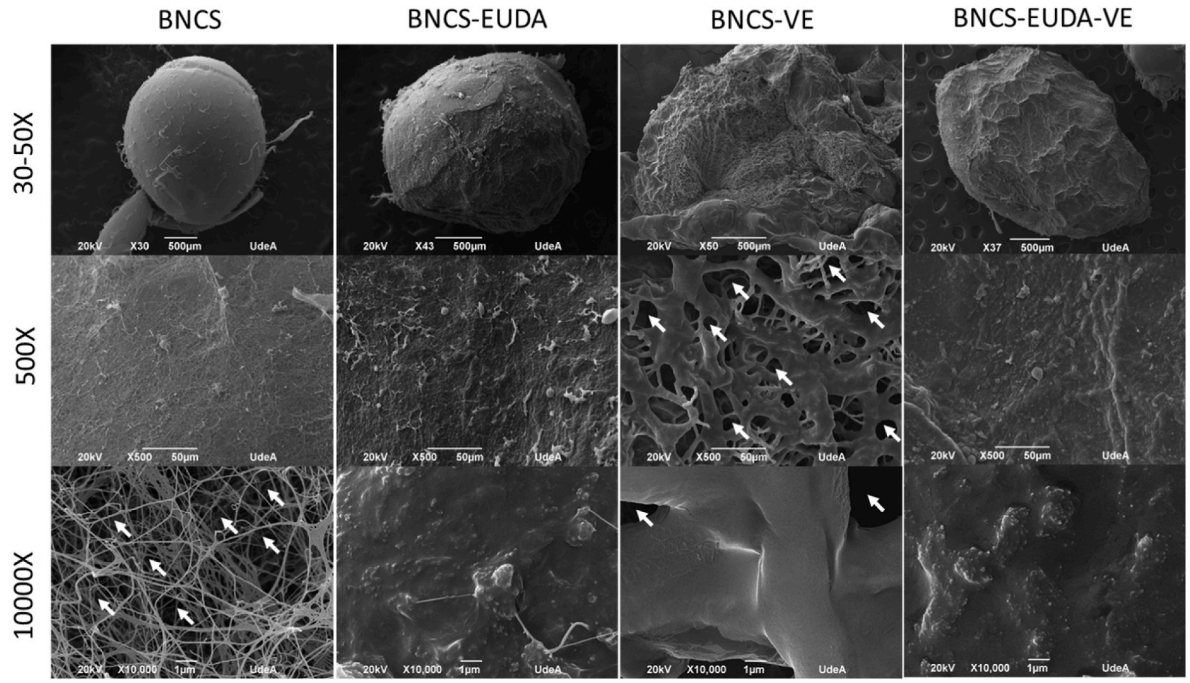

Fig. 3. SEM micrographs of empty capuslies (BNCS ans BNCS-EUDA) and encapsulated VE (BNCS-VE and BNCS-EUDA-VE). Magnifications and scale bars are marked in white in the figure bottom. Arrows indicates reprensentative pores of capsules.

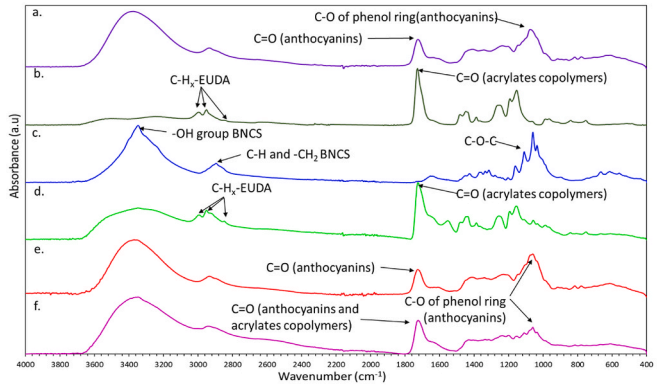

Fig. 4. FTIR-ATR analysis of the bacterial nanocellulose spheres. Individual components: a. VE, b. EUDA and c. BNCS Empty capsules, d. BNCS-EUDA, and VE loaded capsules e. BNCS-VE; f. BNCS-EUDA-VE.

are present. For instance, C═O vibrations bands between 1700 and 1740 cm^{-1}, aromatic bands between 1100 and 1400 cm^{-1}, and C–O vibrations of phenol ring at 1026 cm^{-1} (Barragán Condori et al., 2018), (da Silva et al., 2019). The spectrum of EUDA (Fig. 4 b.) present the bands of acrylates copolymers i.e. the C═O vibrations of carboxylic groups at 1705 cm^{-1} and esterified carboxyl groups at 1730 cm^{-1}, ester vibrations from 1100 to 1200 cm^{-1} and CH$_x$-vibrations from 2900 to 3000 cm^{-1} (Sharma et al., 2011), (Evonik).

The spectrum of the BNCS (see Fig. 4 c.) presents the characteristic bands of cellulose type I allomorphism (Castro et al., 2012; Chiaoprakobkij et al., 2011; Kim et al., 2011b; Shi et al., 2012; Yan et al., 2008), that is, vibrations around 3348 cm^{-1} corresponding to the stretching of the O–H group, bands at 2894 cm^{-1} related to C–H and –CH$_2$ groups, 1642 related to flexion of the OH group of adsorbed water, 1428 cm^{-1} symmetric flexing –CH$_2$ and 1062 cm^{-1} to pyranose C–O-C ring skeletal vibrations (Amin et al., 2014). Other bands at 1374, 1337 cm^{-1}, and 1315 cm^{-1} were attributed to C–H flexion, in-plane O–H flexion, and oscillation of C–H$_2$ groups, indicating the presence of crystalline regions within the structure (Castro et al., 2012).

When coating with EUDA (BNCS-EUDA, in Fig. 4 d.), the bands for the carboxylic groups and CH$_X$-of acrylates copolymers are spotted (El Maghraby et al., 2014), (Thakral et al., 2011), the other bands superimposed with the bands of BNCS, nevertheless, is confirmed the precence of EUDA in the capsules.

In the case of BNCS-VE (Fig. 4 e.), the bands of BCS and VE are superimposed, however, there is still evidence of the presence of C═O and phenols vibrations of anthocynins, confirming the precence of VE in the capsules. Finally, for the full system of BNCS-EUDA-VE (See Fig. 4f) the spectrum shows superimposed bands of the three compounds. For instance, the bands at 1700-1740 cm^{-1} are related to the C═O vibrations of VE and EUDA. The presence of anthocyanins is confirmed via the C–O vibrations at vibrations of phenol ring at 1026 cm^{-1} (Barragán Condori et al., 2018), (da Silva et al., 2019). The other bands are a superimposition of BNCS, EUDA and VE spectrum.

3.3.2. Adsorption isotherm

According to the models presented in Fig. 5, the performance of adsorption isotherms can be described as an incomplete monolayer ($R^2 > 0.99$, for Langmiur, Freundlich, and n-BET models). It can be seen that VE saturates the spheres, reaching a monolayer Langmuir concentration (Q_m) of c. a. 3.37 mg of VE/g BNCS. Additionally, when observing the partition coefficient (K_L) of 1.14 ml/mg VE, it can be concluded that VE has a good affinity and adhesion energy for bacterial nanocellulose, since K_L is greater than 1 ml/mg VE (Sandoval-Ibarra et al., 2015). Going deeper, the n-layer BET equation demonstrates a n_{BET} (number of layers)

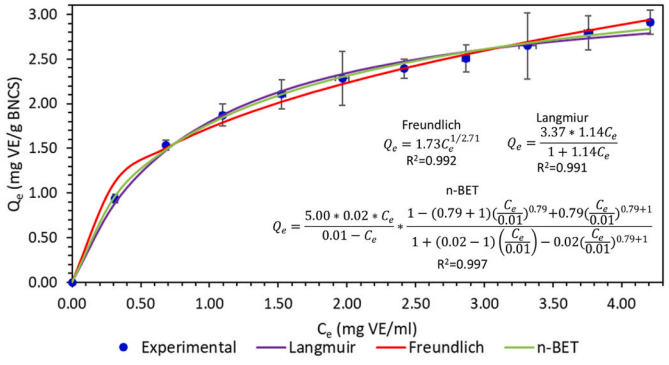

Fig. 5. Adsorption isotherm experiments of VE in BNCS. Indent: Langmuir, Freundlich, and n-BET modeling using quadratic equations and solver. The points are the average of the data and its standard deviation.

of 0.79 (at the monolayer $n_{BET} = 1$ and n-BET equation will be reduced to a Langmuir model (Behere & Yoon, 2021)), confirming the presence of an incomplete monolayer.

3.3.3. Adsorption kinetics

Further analysis of the adsorption kinetics (Fig. 6) for PFO, PSO, and Elovich model shows that the compounds reach the adsorption equilibrium at 60 min. Likewise, VE extracts are coupled to a second-order reaction (see Fig. 6 c.). In this condition, the adsorption rate is dependent on adsorption capacity, not on the concentration of adsorbate (Hussain, 2015), (Anastopoulos & Kyzas, 2014), (Sahoo and Prelot, 2020).

According to the adsorption studies, BNCS can encapsulate c. a. 2.91 mg of VE/g of BNCS, a concentration 5-10-fold above the IC_{50} for cancer cells. Regarding kinetics, the VE adsorption is faster, and the equilibrium is reached during the first hour following a PSO model. The above parameters are important for scaling up the process for future commercialization of derived functional foods.

3.4. Desorption experiments

Fig. 7 shows the experimental coated and uncoated spheres' desorption profiles under gastric conditions (pH = 1.6) and colonic conditions (pH = 7.0). Furthermore, Fig. S2 presents the mathematical modeling of desorption.

The coating of the BNCS greatly influences the VE-releasing profile. Under gastric conditions, the EUDA can reduce an early release of VE by 60% at maximum gastric emptying time (120 min), the equilibrium time is influenced by the capsule type, for BNCS-VE the equilibrium is reahed at 10 min, while for BNCS-EUDA-VE the equilibrium is not reached during the 120 min (maximum desorption of 45.09 ± 4.42%). BNCS-VE can release 72.00 ± 5.09% of VE during the frist 10 min, regarding to the maximum gastric emptying time (120 min) the desorption was 93.09 ± 4.94%. Moreover at stomach eviroment, all the time point are stastically are different between BNCS-VE and BNCS-EUDA-VE indicating that the coarting reduces the desorption of VE (p-value<0.05), These results agree with similar approaches in the literature, where particles and nanoparticles coated with EUDA can reduce colorectal cancer bioactive compounds released under acidic media, which is important to enhance the bioactivity of the drug in the colon (Subudhi et al., 2015).

Under a colonic environment, the behavior of BNCS-EUDA-VE is the opposite, during the first 120 min BNCS-EUDA-VE can deliver faster the load than BNCS-VE, all time points are stastically different, accordingly BNCS-EUDA effectively works as a colorectal drug delivery system for VE. At the end of the average intestinal transit time (4320 min or 72 h) the realease reach c. a. of 70% for both samples.

Regarding to the mathematicall modeling, both capsules behave as a PSO kinetic in both conditions, stomach and colon (see Fig. S3 b, b', e

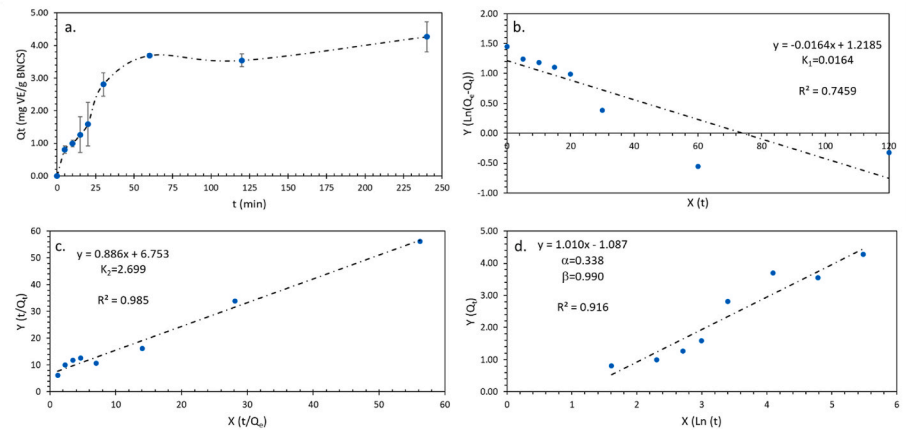

Fig. 6. Adsorption kinetics a. Experimental data, the points are the average of the data and its standard deviation; b. PFO model; c. PSO model; d. Elovich model. The modeling parameters are presented indented in the graphs.

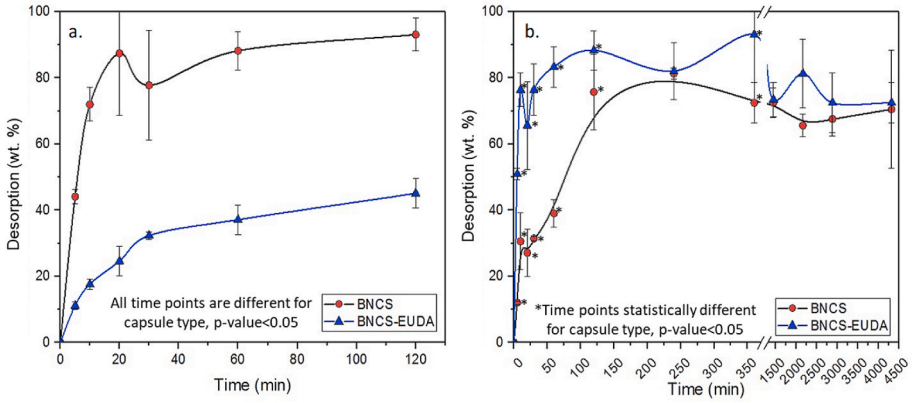

Fig. 7. Experimental desorption profiles of BNCS-VE and BNCS-EUDA-VE, the points are the average of the data and its standard deviation. a. under gastric conditions, annova one-way for each time point, all groups are statiscally different (p-value<0.05); b. under colonic conditions, annova one-way for each time point, groups marked with an asterits (*) are statiscally different (p-value<0.05).

and e'), where the desorption rate is dependent on adsorption capacity, not on the concentration of adsorbate (Hussain, 2015), (Anastopoulos & Kyzas, 2014) (Sahoo and Prelot, 2020). Same behavior as in the adsorption profiles. The above indicates that the delivery profile is influenced by the bacterial nanocellulose, not by EUDA or VE. The hypothesis was confirmed by the similar order of magnitude of the equilibrium rate constant of the PSO model (K_2). Therefore, EUDA influences the amount of VE delivery through changes in the pH and BNC the release rate. Comparing the release behavior, VE is released faster from the BNCS capsules under the stomach than in the colon conditions. Thus, BNCS alone is not recommended as VE colorectal drug delivery system due to the ionic strength of gastric fluids promotes precocious VE delivery (Moore & Scarlata, 1965).

Accordingly, coating BNCS with EUDA is an effective strategy for delivering phytochemicals with potential chemoprevention of colorectal cancer, moreover, bearing in mind that BNCS is GRASS for the FDA, EUDA is a commercially avaible excipient for oral drug delivery system, and Andean berry is an edible fruit.

Nowadays with the grown of knowledge of the potential of phytochemicals for human health is flourishing new stratetegies for developing drug delivery systems of them. In the literature there is reports of several materials such as polysacharides, synthetics materials, extracellular vesicles, proteins, among others to encapsulate phytochemicals for bowel deseases such as curcumin, quercetin, genistein, berberine, among others, for all the cases the phytochemicals performace was enhanced by the use of these materials, due to the enhancement of the oral absorption rate, the solubility, and bioavailability (Castaño et al., 2022), (Rendón et al., 2022), (Li et al., 2023). Comparing with literature, the developed system of BNCS-EUDA improve the bioavailability of VE, as VE can be protected by the capsules under gastric environment and deliver from 5 to 10 fold the IC_{50} of cancer cells while the VE is safe for non-cancereus cells. Limitations of the system should be futher studied using healthy and CRC animals models.

4. Conclusions

A novel system for controlled delivery of VE in BNCS coated with EUDA was developed. The VE demonstrated potential as a phytochemical for colorectal cancer *in vitro,* and it was incorporated into BNCS under a simple and feasible process that can be potentially scaled up for producing functional food ingredients. Moreover, the system discourages the loss/release of VE in gastric conditions as EUDA coating responses to pH. The BNCS demonstrated viability for adsorbing high concentrations of VE, which (5-10-fold above the IC_{50}), once protected using EUDA, can deliver VE 60% of the encapsulated VE under colon conditions. Finally, a synergistic system was designed, in which bacterial nanocellulose generated a proper VE desorption profile while EUDA was a pH-responsive coating that protected it from release at stomach conditions but delivered at the colon. Further studies must be focused on gastrointestinal studies (such as simulated human intestinal microbial ecosystem), sensory analysis (flavor and texture), and food stability to fully understand the system's potential as a functional food ingredient

for beverages and spoonables. Animal cancer models are olso desired to test the potential chemopreventive performance of the system in complex system. Moreover, BNCS (non-coated) should be studied for chemoprevention of stomach cancer, as it can faster deliver phytochemicals under gastric conditions.

Author statement

M.O. and C.C. conceptualized the paper; M.O. designed the experiments; M.O., L. P., V.E., and E. M. performed the experiments; M. O, G. Q and C.C. analyzed the results; J.O., S.P and M.E.M. participated in discussions. M.O. wrote the original draft; all the authors participated in writing-review & editing; C.C. project administration and M.E.M, J.O and C.C funding acquisition.

We would like to confirm that this novel contribution has not been published previously by any of the authors and/or is not under consideration for publication in another journal.

Declaration of competing interest

The authors declare that they have no known competing financial interests or personal relationships that could have appeared to influence the work reported in this paper.

Data availability

No data was used for the research described in the article.

Acknowledgments

This work has been funded by Universidad Pontificia Bolivariana, MINCIENCIAS, MINEDUCACIÓN, MINCIT, and ICETEX through the Program Ecosistema Científico Cod. FP44842-211-2018, project numbers 58674, 58580 y 58536 and the Ministry of Sciences MINCIENCIAS, through the 22 490 Program: NanoBioCáncer 2.0 GAT 2.0. code: 121092092332, grant: 621-2022, projects number 491 92355 and 92391". Moreover, the researchers want to thank Evonik Colombia for donating the Eudragit.

Appendix A. Supplementary data

Supplementary data to this article can be found online at https://doi.org/10.1016/j.foodhyd.2023.109310.

References

Agudelo-Quintero, M. L., Luzardo-Ocampo, I., Lopera-Rodrí Guez, J. A., Maldonado-Celis, M. E., Arango-Varela, S. S., & Co, J. A. L. (2022). Bioactive compounds from andean berry (vaccinium meridio-nale swartz) juice inhibited cell viability and proliferation from SW480 and SW620 human colon adenocarcinoma cells. *Biol. Life Sci. Forum, 2022*, 1–15. https://doi.org/10.3390/xxxxx

Amin, M. C., Abadi, A. G., & Katas, H. (2014). Purification, characterization and comparative studies of spray-dried bacterial cellulose microparticles. *Carbohydrate Polymers, 99*, 180–189. https://doi.org/10.1016/j.carbpol.2013.08.041

Anastopoulos, I., & Kyzas, G. Z. (2014). Agricultural peels for dye adsorption: A review of recent literature. *Journal of Molecular Liquids, 200*(PB), 381–389. https://doi.org/10.1016/j.molliq.2014.11.006

Arango-Varela, S. S., Luzardo-Ocampo, I., & Maldonado-Celis, M. E. (2022a). Andean berry (Vaccinium meridionale Swartz) juice, in combination with Aspirin, displayed antiproliferative and pro-apoptotic mechanisms in vitro while exhibiting protective effects against AOM-induced colorectal cancer in vivo. *Food Research International, 157*, Article 111244. https://doi.org/10.1016/j.foodres.2022.111244

Arango-Varela, S. S., Luzardo-Ocampo, I., & Maldonado-Celis, M. E. (2022b). Andean berry (Vaccinium meridionale Swartz) juice, in combination with Aspirin, displayed antiproliferative and pro-apoptotic mechanisms in vitro while exhibiting protective effects against AOM-induced colorectal cancer in vivo. *Food Research International, 157*. https://doi.org/10.1016/J.FOODRES.2022.111244

Azeredo, H. M. C., Barud, H., Farinas, C. S., Vasconcellos, V. M., & Claro, A. M. (2019a). Bacterial cellulose as a raw material for food and food packaging applications. *Frontiers in Sustainable Food Systems, 3*. https://doi.org/10.3389/fsufs.2019.00007

Azeredo, H. M. C., Barud, H., Farinas, C. S., Vasconcellos, V. M., & Claro, A. M. (2019b). Bacterial cellulose as a raw material for food and food packaging applications. *Frontiers in Sustainable Food Systems, 3*. https://doi.org/10.3389/fsufs.2019.00007. Frontiers Media S.A.

Baby, B., Antony, P., & Vijayan, R. (2017). *Antioxidant and anticancer properties of berries, 58*(15), 2491–2507. https://doi.org/10.1080/10408398.2017.1329198, 10.1080/10408398.2017.1329198.

Barragán Condori, M., Aro Aro, J. M., Huamaní Meléndez, V. J., & Cartagena Cutipa, R. (2018). Antocianinas, compuestos fenólicos y capacidad antioxidante del mio - mio (Coriaria ruscifolia L). *Revista de Investigaciones Altoandinas, 20*(4), 419–428. https://doi.org/10.18271/ria.2018.419

Behere, K., & Yoon, S. (2021). n-Layer BET adsorption isotherm modeling for multimeric Protein A ligand and its lifetime determination. *Journal of Chromatography B, 1162*, Article 122434. https://doi.org/10.1016/J.JCHROMB.2020.122434

Benzie, I. F. F., & Strain, J. J. (1999). Ferric reducing/antioxidant power assay: Direct measure of total antioxidant activity of biological fluids and modified version for simultaneous measurement of total antioxidant power and ascorbic acid concentration. *Methods in Enzymology, 299*(1995), 15–27. https://doi.org/10.1016/S0076-6879(99)99005-5

Brandes, R., Trindade, E., Vanin, D., Vargas, V., Carminatti, C., Al-Qureshi, H., & Recouvreux, D. (2018). Spherical bacterial cellulose/TiO2 nanocomposite with potential application in contaminants removal from wastewater by photocatalysis. Fibers and. *Polymers, 19*(9), 1861–1868. https://doi.org/10.1007/s12221-018-7798-7

Carlos, D. A., Sandra, A., Fabián, C.-M., Benjamín, R., & Maria, E. M. (2017). Antiproliferative and pro-apoptotic effects of Andean berry juice (Vaccinium meridionale Swartz) on human colon adenocarcinoma SW480 cells. *Journal of Medicinal Plants Research, 11*(24), 393–402. https://doi.org/10.5897/jmpr2017.6401

Castaño, M., Martínez, E., Osorio, M., & Castro, C. (2022). Development of genistein drug delivery systems based on bacterial nanocellulose for potential colorectal cancer chemoprevention: Effect of nanocellulose surface modification on genistein adsorption. *Molecules, 27*, 21. https://doi.org/10.3390/molecules27217201

Castro, C., Zuluaga, R., Álvarez, C., Putaux, J-L., Caro, G., Rojas, O., … Gañán, P. (2012). Bacterial cellulose produced by a new acid-resistant strain of Gluconacetobacter genus. *Carbohydrate Polymers, 89*(4), 1033–1037. https://doi.org/10.1016/j.carbpol.2012.03.045

Celis, M. E. M., Tobón, Y. N. F., Agudeio, C., Arango, S. S., & Rojano, B. (2017). Andean berry (vaccinium meridionale swartz). In*Fruit and vegetable phytochemicals: Chemistry and human health* (2nd ed., Vol. 2, pp. 869–881). https://doi.org/10.1002/9781119158042.ch40 November.

Chiaoprakobkij, N., Sanchavanakit, N., Subbalekha, K., Pavasant, P., & Phisalaphong, M. (2011). Characterization and biocompatibility of bacterial cellulose/alginate composite sponges with human keratinocytes and gingival fibroblasts. *Carbohydrate Polymers, 85*(3), 548–553. https://doi.org/10.1016/j.carbpol.2011.03.011

Czaja, W., Romanovicz, D., & malcolm Brown, R. (2004). Structural investigations of microbial cellulose produced in stationary and agitated culture. *Cellulose, 11*(3/4), 403–411. https://doi.org/10.1023/b:cell.0000046412.11983.61

El Maghraby, G. M., Elzayat, E. M., & Alanazi, F. K. (2014). Investigation of in situ gelling alginate formulations as a sustained release vehicle for co-precipitates of dextromethrophan and Eudragit S 100. *Acta Pharmaceutica, 64*(1), 29–44. https://doi.org/10.2478/acph-2014-0002

Evonik. "Eudragit L 100 and Eudragit S 100 specification sheet.". https://healthcare.evonik.com/en/drugdelivery/oral-drug-delivery/oral-excipients/eudragit-portfolio. (Accessed 25 June 2023).

Garzón, G. A., Soto, C. Y., López-R, M., Riedl, K. M., Browmiller, C. R., & Howard, L. (2020). Phenolic profile, in vitro antimicrobial activity and antioxidant capacity of Vaccinium meridionale Swartz pomace. *Heliyon, 6*(5), Article e03845. https://doi.org/10.1016/j.heliyon.2020.e03845

Giusti, M. M., & Wrolstad, R. E. (2001). Characterization and measurement of anthocyanins by UV-visible spectroscopy. *Current Protocols in Food Analytical Chemistry*, (1)https://doi.org/10.1002/0471142913.faf0102s00. F1.2.1-F1.2.13.

Hussain, C. M. (2015). *Carbon nanomaterials as adsorbents for environmental analysis* (Vol. 9781118496). https://doi.org/10.1002/9781118845530.ch14

Indrayanto, G., Putra, G. S., & Suhud, F. (2021). Validation of in-vitro bioassay methods: Application in herbal drug research. *Profiles of Drug Substances, Excipients and Related Methodology, 46*, 273–307. https://doi.org/10.1016/BS.PODRM.2020.07.005

Jarrell, J., Cal, T., & Bennett, J. W. (2000). The Kombucha consortia of yeasts and bacteria. *Mycologist, 14*(4), 166–170. https://doi.org/10.1016/S0269-915X(00)80034-8

Jimenez-Garcia, S. N., Vazquez-Cruz, M., Garcia-Mier, L., Contreras-Medina, L., Guevara-González, R., Garcia-Trejo, J., & Feregrino-Perez, A. (2018). Chapter 13 - phytochemical and pharmacological properties of secondary metabolites in berries. In A. M. Holban, & A. M. Grumezescu (Eds.), *Therapeutic foods* (pp. 397–427). Academic Press. https://doi.org/10.1016/B978-0-12-811517-6.00013-1.

Joseph, S. K., Sabitha, M., & Nair, S. C. (2020). Stimuli-responsive polymeric nanosystem for colon specific drug delivery. *Advanced Pharmaceutical Bulletin, 10*(1), 1–12. https://doi.org/10.15171/apb.2020.001. Tabriz University of Medical Sciences.

Kim, J., Cai, Z., Lee, H. S., Choi, G. S., Lee, D. H., & Jo, C. (2011a). Preparation and characterization of a Bacterial cellulose/Chitosan composite for potential biomedical application. *Journal of Polymer Research, 18*(4), 739–744. https://doi.org/10.1007/s10965-010-9470-9

Kim, J., Cai, Z., Lee, H. S., Choi, G. S., Lee, D. H., & Jo, C. (2011b). Preparation and characterization of a Bacterial cellulose/Chitosan composite for potential biomedical application. *Journal of Polymer Research, 18*(4), 739–744. https://doi.org/10.1007/s10965-010-9470-9

Kumagai, A., Mizuno, M., Kato, N., Nozaki, K., Togawa, E., Yamanaka, S., … Amano, I. (2011). Ultrafine cellulose fibers produced by Asaia bogorensis, an acetic acid

bacterium. *Biomacromolecules, 12*(7), 2815–2821. https://doi.org/10.1021/bm2005615

Li, N., Wang, M., Lyu, Z., Shan, K., Chen, Z., Chen, B., … Li, H. (2023). Medicinal plant-based drug delivery system for inflammatory bowel disease. *Frontiers in Pharmacology, 14*. Frontiers Media S.A.

Maldonado-Celis, M. E., Arango-Varela, S. S., & Rojano, B. A. (2014a). Free radical scavenging capacity and cytotoxic and antiproliferative effects of Vaccinium meridionale Sw. agains colon cancer cell lines. *Revista Cubana de Plantas Medicinales, 19*(2), 172–184.

Maldonado-Celis, M. E., Arango-Varela, S. S., & Rojano, B. A. (2014b). Free radical scavenging capacity and cytotoxic and antiproliferative effects of Vaccinium meridionale Sw. agains colon cancer cell lines. *Revista Cubana de Plantas Medicinales, 19*(2), 172–184 [Online] http://www.medigraphic.com/pdfs/revcubplamed/cpm-2014/cpm142f.pdf.

Maldonado, M. E., Agudelo, C., Varela, S. A., & Rojano, B. (2017). *Andean berry (Vaccinium meridionale swartz)* [Online]. Available: https://www.researchgate.net/publication/320973018.

Marques, M. R. C., Loebenberg, R., & Almukainzi, M. (2011). Simulated biological fluids with possible application in dissolution testing. *Dissolution Technologies, 18*(3), 15–28.

Martínez Ávila, H., Schwarz, S., Feldmann, E. M., Mantas, A., Bomhard, A., Gatenholm, P., & Rotter, N. (2014). Biocompatibility evaluation of densified bacterial nanocellulose hydrogel as an implant material for auricular cartilage regeneration. *Applied Microbiology and Biotechnology, 98*(17), 7423–7435. https://doi.org/10.1007/s00253-014-5819-z

Martínez, E., Osorio, M., Finkielstein, C., Ortíz, I., Peresin, M. S., & Castro, C. (2022). 5-Fluorouracil drug delivery system based on bacterial nanocellulose for colorectal cancer treatment: Mathematical and in vitro evaluation. *International Journal of Biological Macromolecules, 220*, 802–815. https://doi.org/10.1016/j.ijbiomac.2022.08.102

Mehta, R., Chawla, A., Sharma, P., & Pawar, P. (2013). Formulation and in vitro evaluation of Eudragit S-100 coated naproxen matrix tablets for colon-targeted drug delivery system. *\"Journal of Advanced Pharmaceutical Technology & Research\"\"\", 4*(1), 31–41. https://doi.org/10.4103/2231-4040.107498

Molina-Ramírez, C., Zuluaga, R., Castro, C., & Gañán, P. (2018). *Statistical optimization of culture conditions to improve cell density of komagataeibacter medellinensis NBRC 3288: The first step towards to optimize bacterial cellulose production*, Article 381186. https://doi.org/10.1101/381186. bioRxiv.

Moore, E. W., & Scarlata, R. W. (1965). The determination of gastric acidity by the glass electrode. *Gastroenterology, 49*(2), 178–188. https://doi.org/10.1016/s0016-5085(19)34564-0

Okiyama, A., Motoki, M., & Yamanaka, S. (1993). Bacterial cellulose IV. Application to processed foods. *Food Hydrocolloids, 6*(6), 503–511. https://doi.org/10.1016/S0268-005X(09)80074-X

Osorio, M., Castro, C., Velásquez-Cock, J., Vélez-Acosta, L., Cáracamo, L., Sierra, S., Klaiss, R., Avendaño, D., Correa, C., Gómez, C., Zuluaga, R., Builes, D., & Gañán, P. (2017). *Bacterial cellulose nanoribbons: A new bioengineering additive for biomedical and food applications*. https://doi.org/10.1007/978-3-319-61288-1_6

Pircher, N., Veigel, S., Aigner, N., Nedelec, J. M., Rosenau, T., & Liebner, F. (2014). Reinforcement of bacterial cellulose aerogels with biocompatible polymers. *Carbohydrate Polymers, 111*, 505–513. https://doi.org/10.1016/j.carbpol.2014.04.029

Ratner, B. D., Hoffman, A. S., Schoen, F. J., & Lemons, J. E. (2013). *Biomaterials science an introduction to materials in medicine*. Amsterdam: Elsevier. https://doi.org/10.1016/B978-0-08-087780-8.00153-4

Recouvreux, D. O. S., Rambo, C. R., Berti, F. V., Carminatti, C.a., Antônio, R. V., & Porto, L. M. (2011). Novel three-dimensional cocoon-like hydrogels for soft tissue regeneration. *Materials Science and Engineering: C, 31*(2), 151–157. https://doi.org/10.1016/j.msec.2010.08.004

Rendón, J. P., Cañas, A. I., Correa, E., Bedoya-Betancur, V., Osorio, M., Castro, C., & Naranjo, T. W. (2022). Evaluation of the effects of genistein in vitro as a chemopreventive agent for colorectal cancer—strategy to improve its efficiency when administered orally. *Molecules, 27*, 20. https://doi.org/10.3390/molecules27207042

Sahoo, T. R., & Prelot, B. (2020). *Adsorption processes for the removal of contaminants from wastewater: The perspective role of nanomaterials and nanotechnology," Nanomaterials for the Detection and Removal of wastewater pollutants* (pp. 161–222). https://doi.org/10.1016/B978-0-12-818489-9.00007-4

Sandoval-Ibarra, F. D., López-Cervantes, J. L., & Gracia-Fadrique, J. (2015). Ecuación de Langmuir en líquidos simples y tensoactivos. *Educación Química, 26*(4), 307–313. https://doi.org/10.1016/j.eq.2015.03.002

Sebaugh, J. L. (2011). Guidelines for accurate EC50/IC50 estimation. *Pharmaceutical Statistics, 10*(2), 128–134. https://doi.org/10.1002/pst.426

Sharma, M., Sharma, V., Panda, A. K., & Majumdar, D. K. (2011). Development of enteric submicron particle formulation of papain for oral delivery. *International Journal of Nanomedicine, 6*, 2097–2111. https://doi.org/10.2147/ijn.s23985

Shi, Z., Zang, S., Jiang, F., Huang, L., Lu, D., Ma, Y., & Yang, G. (2012). In situ nano-assembly of bacterial cellulose–polyaniline composites. *RSC Advances, 2*(1), 1040–1046. https://doi.org/10.1039/c1ra00719j

Shi, X., Ye, Y., Wang, H., Liu, F., & Wang, Z. (2018). Designing pH-responsive biodegradable polymer coatings for controlled drug release via vapor-based route. *ACS Applied Materials & Interfaces, 10*(44), 38449–38458. https://doi.org/10.1021/acsami.8b14016

Shi, Z., Zhang, Y., Phillips, G. O., & Yang, G. (2014). Utilization of bacterial cellulose in food. *Food Hydrocolloids, 35*, 539–545. https://doi.org/10.1016/j.foodhyd.2013.07.012

da Silva, H. R., Assis, D. C., Prada, A. L, Silva, J. O. C., Sousa, M. B., Ferreira, A. M., Amado, J. R. R., Carvalho, H., dos Santos, A., & Carvalho, J. (2019). Obtaining and characterization of anthocyanins from Euterpe oleracea (açaí) dry extract for nutraceutical and food preparations. *Revista Brasileira de Farmacognosia, 29*(5), 677–685. https://doi.org/10.1016/j.bjp.2019.03.004

Spence, C. (2015). On the psychological impact of food colour. *Flavour, 4*(1), 1–16. https://doi.org/10.1186/s13411-015-0031-3

Subudhi, B. M., Jain, A., Jain, A., Hurkat, P., Shilpi, S., Gulbake, A., & Jain, S. (2015). Eudragit S100 coated citrus pectin nanoparticles for colon targeting of 5-fluorouracil. *Materials, 8*(3). https://doi.org/10.3390/ma8030832

Thakral, N. K., Ray, A. R., Bar-Shalom, D., Eriksson, A. H., & Majumdar, D. K. (2011). The quest for targeted delivery in colon cancer: Mucoadhesive valdecoxib microspheres. *International Journal of Nanomedicine, 6*, 1057–1068. https://doi.org/10.2147/ijn.s19561. May 2014.

Trovatti, E., Silva, N. H., Duarte, I., Rosado, C. F., Almeida, I., Costa, P., Freire, S. R., Silvestre, A., & Neto, C. (2011). Biocellulose membranes as supports for dermal release of lidocaine. *Biomacromolecules, 12*(11), 4162–4168. https://doi.org/10.1021/bm201303r

Yahfoufi, N., Alsadi, N., Jambi, M., & Matar, C. (2018). The immunomodulatory and anti-inflammatory role of polyphenols. *Nutrients, 10*(11). https://doi.org/10.3390/nu10111618. MDPI AG.

Yan, Z., Chen, S., Wang, H., Wang, B., & Jiang, J. (2008). Biosynthesis of bacterial cellulose/multi-walled carbon nanotubes in agitated culture. *Carbohydrate Polymers, 74*(3), 659–665. https://doi.org/10.1016/j.carbpol.2008.04.028

Yudianti, R., & Karina, M. (2012). Development of nanocomposites from bacterial cellulose and poly(vinyl alcohol) using casting-drying method. *Procedia Chemistry, 4*(2), 73–79. https://doi.org/10.1016/j.proche.2012.06.011

Zhang, T., Ma, C., Zhang, Z., Zhang, H., & Hu, H. (2021). NF-κB signaling in inflammation and cancer. *MedComm (Beijing), 2*(4), 618. https://doi.org/10.1002/MCO2.104

Zhu, H., Jia, S., Wan, T., Jia, Y., Yang, H., Li, J., Yan, L., & Zhong, C. (2011b). Biosynthesis of spherical Fe3O4/bacterial cellulose nanocomposites as adsorbents for heavy metal ions. *Carbohydrate Polymers, 86*(4), 1558–1564. https://doi.org/10.1016/j.carbpol.2011.06.061

Zhu, H., Jia, S., Yang, H., Jia, Y., Yan, L., & Li, J. (2011). Preparation and application of bacterial cellulose sphere: A novel biomaterial. *Biotechnology & Biotechnological Equipment, 25*(1), 2233–2236. https://doi.org/10.5504/bbeq.2011.0010